HHS Public Access

Author manuscript

J Am Chem Soc. Author manuscript; available in PMC 2019 October 24.

Published in final edited form as:

J Am Chem Soc. 2018 October 24; 140(42): 13550–13553. doi:10.1021/jacs.8b07866.

Site-Specific Labeling of Cyanine and Porphyrin Dye-Stabilized Nanoemulsions with Affibodies for Cellular Targeting

Ahmad Amirshaghaghi[†], **Burcin Altun**[†], **Kido Nwe**[‡], **Lesan Yan**[†], **Joel M. Stein**[†,§], **Zhiliang Cheng**[†], and **Andrew Tsourkas**[†]

[†]Department of Bioengineering, School of Engineering and Applied Sciences, University of Pennsylvania, Philadelphia, Pennsylvania 19104, United States

[‡]Chemical and Nanoparticle Synthesis Core, University of Pennsylvania, Philadelphia, Pennsylvania 19104, United States

[§]Department of Radiology, Division of Neuroradiology, Hospital of the University of Pennsylvania, Philadelphia, Pennsylvania 19104, United States

Abstract

Recently, it has been shown that amphiphilic dyes such as Indocyanine Green (ICG) and Protoporphyrin IX (PpIX) can solubilize hydrophobic colloids and/or drugs by driving the formation of stable nanoemulsions. These nanoemulsions are unique in that they can be composed entirely of functional and clinically-used materials; however, they lack bio-orthogonal chemical handles for the facile attachment of targeting ligands. The ability to target nanoparticles is desirable because it can lead to improved specificity and reduced side effects. Here, we describe variants of ICG and PpIX with azide handles that can be readily incorporated into dye-stabilized nanoemulsions and facilitate the attachment of targeting ligands via click-chemistry in a simple, scalable and reproducible reaction. As a model system, an anti-Her2 affibody was site-specifically attached to both ICG and PpIX-stabilized nanoemulsions with encapsulated superparamagnetic iron oxide nanoparticles.

Table of Contents Figure

Corresponding Author, atsourk@seas.upenn.edu.

Notes

The authors declare no competing financial interest.

ASSOCIATED CONTENT

Supporting Information

The Supporting Information is available free of charge on the ACS Publications website.

Methods and instruments, Explaining synthesis routs (section S1), and Figures S1–S9 (PDF).

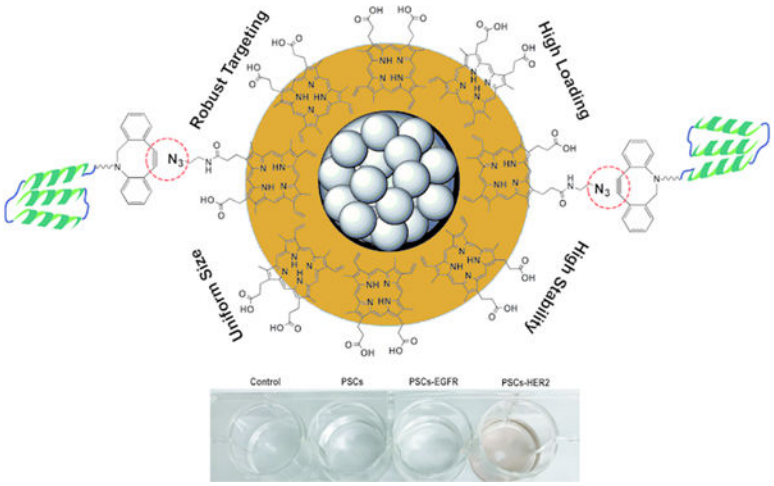

Nanoparticles have recently garnered a significant amount of attention as a platform for drug delivery because of their ability to reduce off-target effects, extend drug circulation, and improve the treatment of disease.[1–3] This has led to the development of a diverse array of nanocarriers, which include liposomes; dendrimers; polymeric micelles; silica; metallic nanoparticles (e.g. silver, gold, iron oxide); and carbon nanotubes.[4–6] Almost all currently existing nanocarriers require the use of carrier materials, such as amphiphiles, to solubilize their cargo. Recently, we introduced a new class of nanoparticles, whereby amphiphilic functional dyes such as the near-infrared fluorescent dye Indocyanine Green (ICG) and the photosensitizer Protoporphyrin IX (PpIX) (i.e., clinically-used functional materials) are used to drive the formation of stable nanoemulsions, without the use of any additional amphiphilic polymers, lipids, or surfactants.[7,8] Hydrophobic materials such as superparamagnetic iron oxide nanoparticles (SPIONs) can be encapsulated in the nanoemulsions to confer additional functionality. It has also been shown that small-molecule hydrophobic drugs can be packaged into nanoemulsions using a similar approach.[9] These novel dyestabilized nanoemulsions allow for extremely high drug payloads and have been shown to exhibit improved efficacy compared with free drug [9] and even analogous micelle carriers, due to their exceptional stability and reduced drug leakage.[8]

The attachment of targeting ligands to nanoparticles is desirable because it has the potential to increase both tumor accumulation and specificity, and ultimately the therapeutic index.[10–12] While many nanoparticles rely primarily on enhanced permeability and retention (EPR) for preferential accumulation at tumor sties,[13] active targeting is generally preferred to more specifically deliver drugs to the desired cell type based on its molecular profile through ligand-receptor or antibody-antigen interactions.[14,15] Targeting has also been shown to trigger cellular uptake for more effective delivery of drug to intracellular targets.[16–18] Despite the benefits of targeting, low bioconjugation efficiencies, high batch-to-batch variability, and the inability to control the orientation and density of the targeting ligands on the nanoparticle surface slows clinical translation.[9,19,20]

Dye-stabilized nanoemulsions have yet to be functionalized with any disease-associated targeting ligands. The surface chemistry and chemical handles available for bioconjugation

are dependent on the dye used and for some dyes no chemical handle is available for subsequent bioconjugations. Preferably, a bioorthogonal chemical handle would be available for the attachment of targeting ligands via click-chemistry.[21] Click chemistry is a highly efficient and specific reaction chemistry that has become the preferred approach for bioconjugations. One of the most popular click chemistry reactions occurs between an azide and a constrained alkyne, with efficiencies nearing 100%, without copper catalysts.[22] Herein, we describe a strategy for the site-specific and efficient attachment of targeting ligands onto carrier-free, ICG- and PpIX-stabilized nanoemulsions.

Azide-handles for click-chemistry were introduced onto the surface of dye-stabilized nanoemulsions, by first preparing azidemodified variants of ICG and PpIX (Figure 1). The azide was introduced near the hydrophilic sulfate and carboxyl groups of ICG and PpIX, respectively, to increase the likelihood that it would be exposed to the surrounding aqueous medium and available for subsequent conjugations. The structure of the azide variants was confirmed by ESI-MS and ^{1}H NMR (Supporting information, Section S1 and Figure S1). The absorbance and fluorescence spectra of the azide variants and the free dyes (in DMSO) were identical (Figure S2). Azide-functionalized nanoemulsions were formed by first dissolving the azide-dyes at a 1:20 molar ratio with unmodified dye in Dimethyl sulfoxide (DMSO). This dye mixture was combined with SPION (SPIONs, diameter = 7.6 ± 1.0 nm; Figure S3) in toluene at a ratio of 1:1 w/w. No additional amphiphiles or carrier materials were applied. The sample was sonicated in water to form the nanoemulsion and purified by dialysis. The amphiphilic ICG-N_3/ICG and PpIX-N_3/PpIX mixtures solubilized the hydrophobic SPIONs, creating stable ICG-SPION-N_3 nanoemulsions (ISCs-N_3) and PpIX-SPION-N_3 nanoemulsions (PSCs-N_3), respectively. The average hydrodynamic diameter of the ISCs-N_3 and PSCs-N_3 was 58 ± 4.3 nm and 50 ± 3.6 nm respectively. The average polydispersity index (PDI) was <0.2 for both formulations (Figure 2B and S4A).

Anti-Her2 targeting affibodies were used as a model targeting ligand and were site-specifically labeled at the C-terminus with a constrained alkyne, dibenzocyclooctyne (DBCO), via sortase-tag expressed protein ligation (STEPL).[23] Briefly, the affibody was expressed as a fusion protein with the sortase-recognition motif, sortase, and a histidine affinity tag. Once captured on affinity resin, the addition of a triglycine peptide modified with DBCO, led to the sortase mediation ligation of the peptide onto the affibody and release of the anti-Her2 affibody-DBCO conjugate (HER2DBCO) from the column (Figure S5).

Affibody-targeted nanoemulsions (Figure 2A) were then prepared by simply mixing the HER2-DBCO with either the ISCs-N_3 or the PSCs-N_3 to produce HER2-targeted nanoemulsions (ISCsHER2 and PSCs-HER2). After conjugation, the average hydrodynamic size of the ISCs-HER2 and PSCs-HER2 was increased to around 78 ± 5 nm and 60 ± 7 nm, respectively (Figure 2B and S4A). The average polydispersity index (PDI) was <0.2 for both formulations. Images acquired by transmission electron microscopy (TEM) confirmed the formation of tightly packed SPION nanoemulsions with a narrow size distribution (Figure 2C and S4B). PSCs-HER2 and ISCs-HER2 were found to be highly stable in water with no signs of aggregation or precipitation, as indicated by no significant changes in the T_2 relaxation time (Figure S6A and S6C) or hydrodynamic diameter over the course of at least

6 days. Relaxometry measurements indicated an average r_2 value of 360 ± 4 and 390 ± 6 mM^{-1} s^{-1} for PSCs-HER2 and ISCs-HER2, respectively (Figure S6B and S6D).

The cytotoxicity of the PSCs-HER2 and ISCs-HER2 were examined in an MTS cell proliferation assay. Increasing concentrations of targeted-nanoemulsions were incubated with HER2/neu-positive breast cancer cells (T6–17). It was found that the targeted-nanoemulsions exhibited no significant cytotoxicity up to a concentration of 125 ug/mL (Figure S7).

To investigate binding of the nanoemulsions to target cells, PSCs-HER2 were incubated with HER2-positive, EGFR-negative T617 breast cancer cells for 1 hr. The cells were then washed and imaged by phase contrast and fluorescence microscopy (Figure 3A). Negative control studies were performed with PSCs that had not been functionalized with any targeting ligands as well as PSCs labeled with an anti-EGFR affibody. All studies were performed at equivalent concentrations of PpIX (6 ug/ml). Little to no cellular fluorescence was observed following incubation of T617 cells with either PSCs-EGFR or unlabeled PSCs. In contrast, a bright fluorescence signal was observed when T617 cells incubated with the PSCs-HER2. We obtained similar results when T617 cells were incubated with ISCs-HER2 and the analogous negative controls (Figure S8A).

To confirm that the HER2 affibody-dye conjugate was not dissociating from the nanoemulsion, labeled T617 cells were also assessed by magnetic resonance. For these studies, all experiments were performed at equivalent concentrations of iron (100 ug/mL) and nanoemulsions were incubated with cells for 1 hr.

Only a slight reduction in the T_2 relaxation time of T617 cells was observed following incubation with PSCs-EGFR and the nontargeted PSCs, indicative of little to no nonspecific binding (Figure 3B). Similar results were observed with ISCs-EGFR and nontargeted ISCs (Figure S8B). In contrast, the T617 cells that were incubated with the PSCs-HER2 or ISCs-EGFR exhibited a significantly lower T_2 relaxation time, which is indicative of the presence of SPION. MR imaging of the cell samples confirmed strong T_2 contrast for cells labeled with the targeted nanoemulsions, relative to the negative controls (Figure 3C and S8C).

Binding of the PSCs-HER2 was even evident by visual inspection of the monolayer of T617 cells in 12-well plates, after several washes with PBS to remove unbound nanoemulsions (Figure 3D). Therefore, these results provide clear evidence that affibodytargeted nanoemulsions specifically bind to HER2/neu-positive cells and the targeting ligands remains associated with the nanoemulsions.

Finally, to confirm that the affibodies were covalently conjugated to the nanoemulsions and not passively adsorbed, ISCs and PSCs without azide handles were mixed with DBCO-HER2, following the same experimental conditions as when ISCs-N_3 and PSCs-N_3 were used. It was found that there was no significant difference between the non-targeted nanoemolsions and the nanoemolsions mixed with affibodies, when incubated with T617 cells and analyzed by fluorescence microscopy and magnetic resonance (Figure S9). These findings suggest that it is necessary to covalently attach the affibodies to the nanoemulsions to achieve effective targeting.

In summary, we demonstrated that dye-stabilized nanoemulsions can be functionalized with targeting ligands. We developed a versatile and easy-to-operate conjugation method that uses click chemistry for the efficient attachment of targeting ligands to the surface of the nanoemulsions. These particles are highly stable, allow for high loading of dyes, and display high relaxivity. We believe that our affibody conjugation strategy, using catalyst-free click chemistry, can be applied to diverse applications such as molecular imaging, drug delivery, and photodynamic therapy.

Supplementary Material

Refer to Web version on PubMed Central for supplementary material.

ACKNOWLEDGMENT

This work was supported in part by the National Institutes of Health R01CA181429 (A.T.), R01NS100892 (Z.C.), and R01CA175480 (Z.C.)

REFERENCES

(1). Senapati S; Mahanta AK; Kumar S; Maiti P Controlled Drug Delivery Vehicles for Cancer Treatment and Their Performance. Signal Transduct. Target. Ther 2018, 3 (1), 1–19.

(2). Chen H; Zhang W; Zhu G; Xie J; Chen X Rethinking Cancer Nanotheranostics. Nat. Rev. Mater 2017, 2, 17024. [PubMed: 29075517]

(3). Davis ME; Chen Z; Shin DM Nanoparticle Therapeutics: An Emerging Treatment Modality for Cancer. Nat. Rev. Drug Discov 2008, 7 (9), 771–782. [PubMed: 18758474]

(4). Torchilin VP Multifunctional, Stimuli-Sensitive Nanoparticulate Systems for Drug Delivery. Nat. Rev. Drug Discov 2014, 13 (11), 813–827. [PubMed: 25287120]

(5). Zhang J; Yuan ZF; Wang Y; Chen WH; Luo GF; Cheng SX; Zhuo RX; Zhang XZ Multifunctional Envelope-Type Mesoporous Silica Nanoparticles for Tumor-Triggered Targeting Drug Delivery. J. Am. Chem. Soc 2013, 135 (13), 5068–5073. [PubMed: 23464924]

(6). Singh R; L. J W. Nanoparticle-Based Targeted Drug Delivery. Exp. Mol .Pathol 2009, 86 (3), 215–223. [PubMed: 19186176]

(7). Thawani JP; Amirshaghaghi A; Yan L; Stein JM; Liu J; Tsourkas A Photoacoustic-Guided Surgery with Indocyanine Green-Coated Superparamagnetic Iron Oxide Nanoparticle Clusters. Small 2017, 13 (37), 1–9.

(8). Yan L; Amirshaghaghi A; Huang D; Miller J; Stein JM; Busch TM; Cheng Z; Tsourkas A Protoporphyrin IX (PpIX)Coated Superparamagnetic Iron Oxide Nanoparticle (SPION) Nanoclusters for Magnetic Resonance Imaging and Photodynamic Therapy. Adv. Funct. Mater 2018, 28, 1–8.

(9). Shamay Y; Shah J; Işlk M; Mizrachi A; Leibold J; Tschaharganeh DF; Roxbury D; Budhathoki-Uprety J; Nawaly K; Sugarman JL; et al. Quantitative Self-Assembly Prediction Yields Targeted Nanomedicines. Nat. Mater 2018, 17 (4), 361–368. [PubMed: 29403054]

(10). Bazak R; Houri M; El Achy S; Kamel S; Refaat T Cancer Active Targeting by Nanoparticles: A Comprehensive Review of Literature. J. Cancer Res. Clin. Oncol 2015, 141 (5), 769–784. [PubMed: 25005786]

(11). Conway CL; Walker I; Bell A; Roberts DJH; Brown SB; Vernon DI In Vivo and in Vitro Characterisation of a Protoporphyrin IX–cyclic RGD Peptide Conjugate for Use in Photodynamic Therapy. Photochem. Photobiol. Sci 2008, 7 (3), 290–298. [PubMed: 18389145]

(12). Ruoslahti E; Bhatia SN; Sailor MJ Targeting of Drugs and Nanoparticles to Tumors. J. Cell Biol 2010, 188 (6), 759–768. [PubMed: 20231381]

(13). Ngoune R; Peters A; von Elverfeldt D; Winkler K; Pütz G Accumulating Nanoparticles by EPR: A Route of No Return. J. Control. Release 2016, 238, 58–70. [PubMed: 27448444]

(14). Mohanraj VJ; Chen Y Nanoparticles – A Review. Trop. J. Pharm. Res 2006, 5, 561–573.

(15). Byrne JD; Betancourt T; Brannon-Peppas L Active Targeting Schemes for Nanoparticle Systems in Cancer Therapeutics. Adv. Drug Deliv. Rev 2008, 60 (15), 1615–1626. [PubMed: 18840489]

(16). Kono K; Takashima M; Yuba E; Harada A; Hiramatsu Y; Kitagawa H; Otani T; Maruyama K; Aoshima S Multifunctional Liposomes Having Target Specificity, Temperature-Triggered Release, and near-Infrared Fluorescence Imaging for Tumor-Specific Chemotherapy. J. Control. Release 2015, 216, 69–77. [PubMed: 26264832]

(17). Zhang K; Hao L; Hurst SJ; Mirkin CA Antibody-Linked Spherical Nucleic Acids for Cellular Targeting. J. Am. Chem. Soc 2012, 134 (40), 16488–16491. [PubMed: 23020598]

(18). Elias DR; Cheng Z; Tsourkas A An Intein-Mediated SiteSpecific Click Conjugation Strategy for Improved Tumor Targeting of Nanoparticle Systems. Small 2010, 6 (21), 2460– 2468. [PubMed: 20925038]

(19). Beck A; Goetsch L; Dumontet C; Corvaïa N Strategies and Challenges for the next Generation of Antibody-Drug Conjugates. Nat. Rev. Drug Discov 2017, 16 (5), 315–337. [PubMed: 28303026]

(20). Vargo KB; Zaki A. Al; Warden-Rothman R; Tsourkas A; Hammer DA Superparamagnetic Iron Oxide Nanoparticle Micelles Stabilized by Recombinant Oleosin for Targeted Magnetic Resonance Imaging. Small 2015, 11 (12), 1409–1413. [PubMed: 25418741]

(21). Baskin JM; Prescher JA; Laughlin ST; Agard NJ; Chang PV; Miller IA; Lo A; Codelli JA; Bertozzi CR Copper-Free Click Chemistry for Dynamic in Vivo Imaging. Proc. Natl. Acad. Sci 2007, 104 (43), 16793–16797. [PubMed: 17942682]

(22). Hao J; Huang LL; Zhang R; Wang HZ; Xie HY A Mild and Reliable Method to Label Enveloped Virus with Quantum Dots by Copper-Free Click Chemistry. Anal. Chem 2012, 84 (19), 8364–8370. [PubMed: 22946933]

(23). Warden-Rothman R; Caturegli I; Popik V; Tsourkas A Sortase-Tag Expressed Protein Ligation: Combining Protein Purification and Site-Specific Bioconjugation into a Single Step. Anal. Chem 2013, 85 (22), 11090–11097. [PubMed: 24111659]

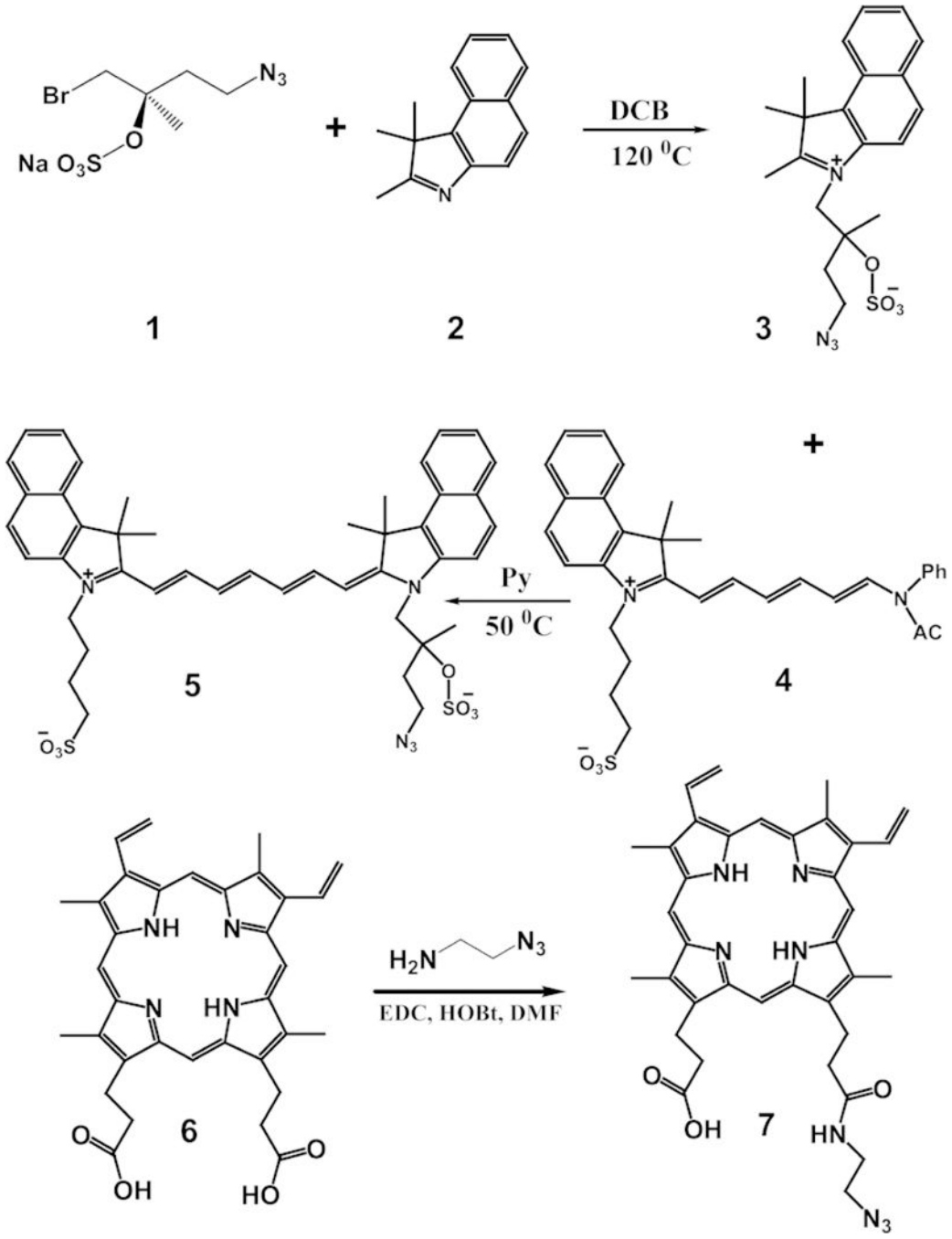

Figure 1.
Synthetic route of the ICG-N_3 (compound 5) and PpIX-N_3 (compound 7).

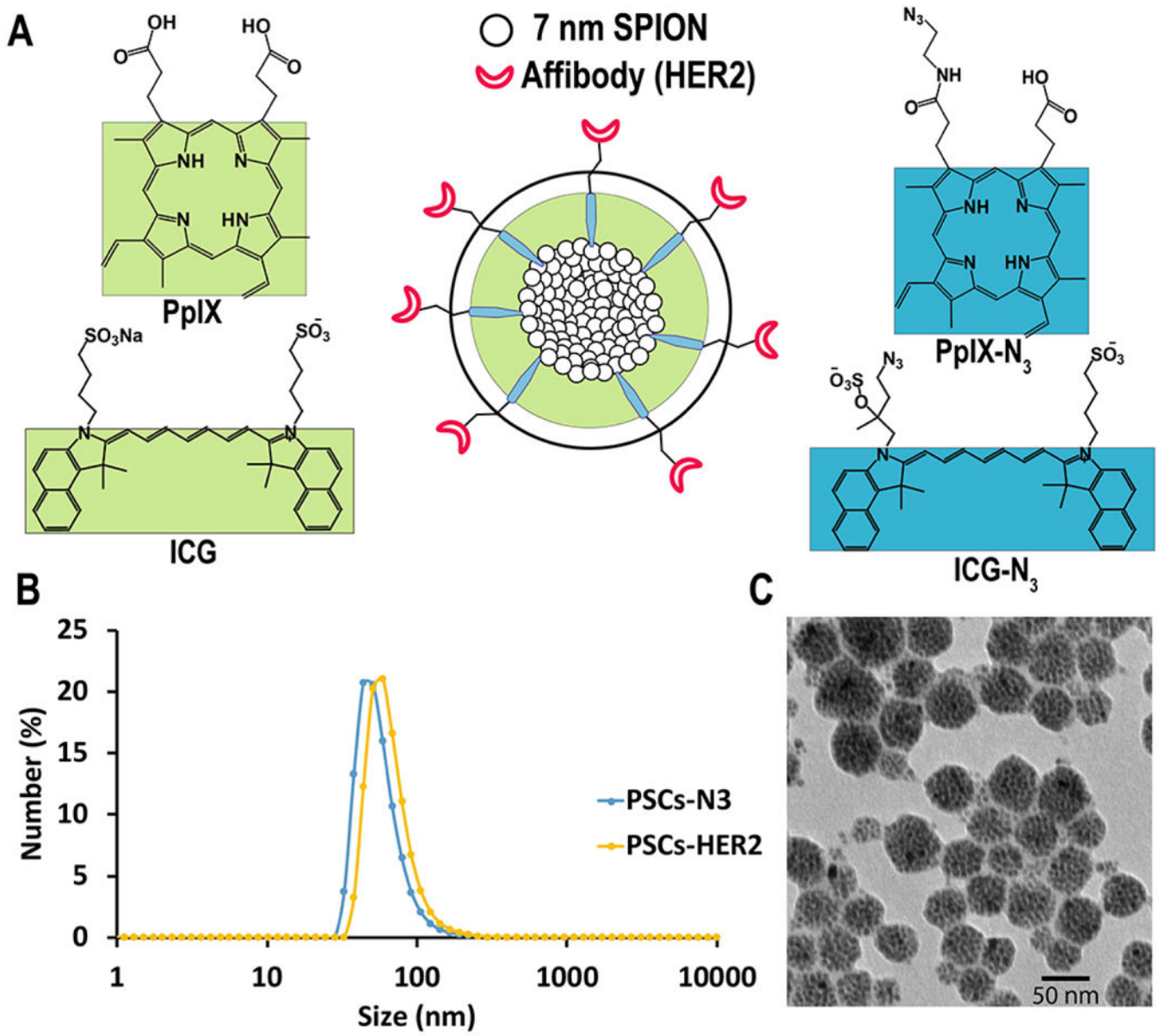

Figure 2.

(A) Schematic of a targeted, ICG- or PpIX-stabilized nanoemulsion (i.e., PpIX-N_3/PpIX or ICG-N_3/ICG, Blue/Green) with hydrophobic SPIONs encapsulated in the core. (B) Dynamic light scattering (DLS) of PSCs-N_3 (50 ± 3.6 nm) and PSCs-HER2 (60 ± 7 nm) in water. (C) TEM image of PSCs-HER2 shows tightly packed SPIONs within the nanoemulsions (scale bar: 50 nm).

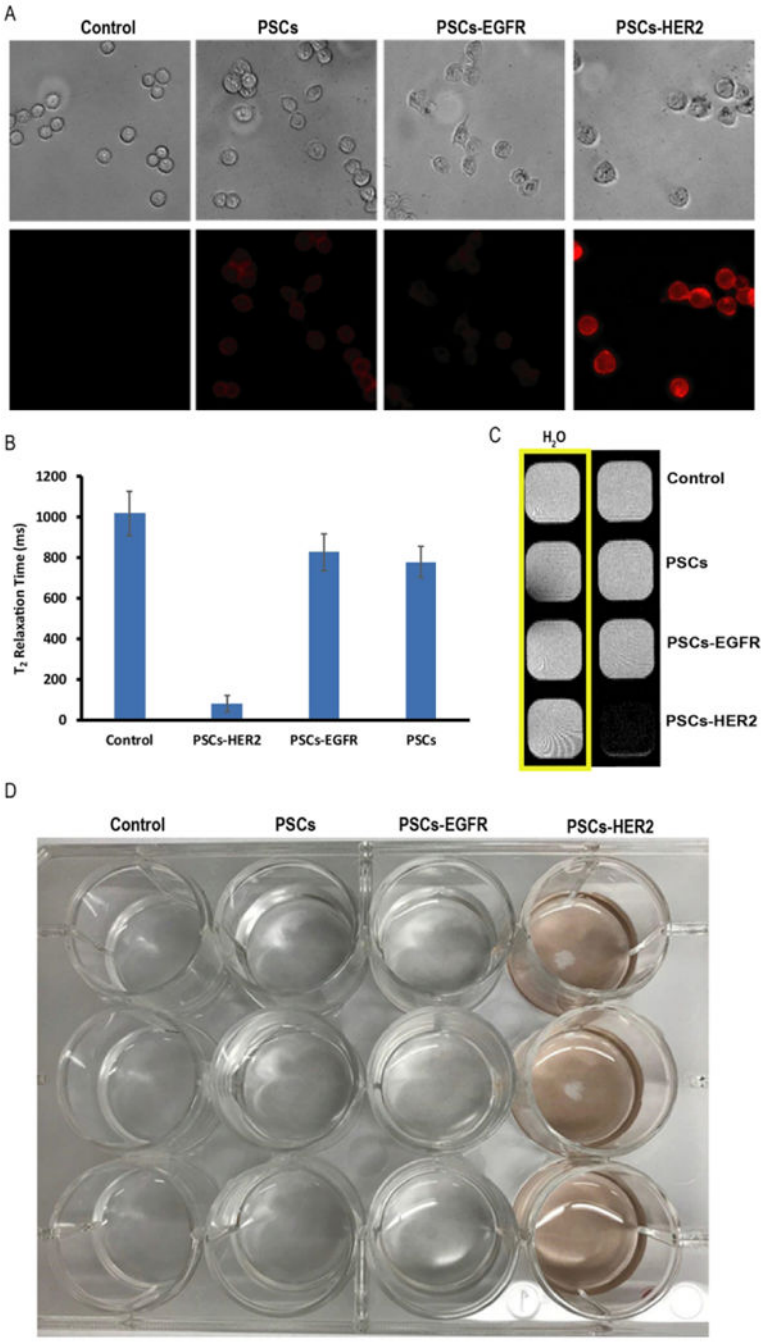

Figure 3.

(A) Phase contrast (top row) and fluorescence microscopy (bottom row) images of HER2/neu-positive T617 cells incubated without nanoemulsions (control) and with PSCs, PSCsEGFR and PSCs-HER2 for 1h. (B) Relaxivity measurements of T617 cells incubated with targeted and non-targeted nanoemulsions. (C) MR phantom image of T617 cells after incubation with targeted and non-targeted PSCs for 1h. (D) Photograph of T617 cells in a 12 well-plate following incubation with targeted and non-targeted PSCs.